Likelihood, Bayesian, Inference and Their Application to the Solution of New Structures

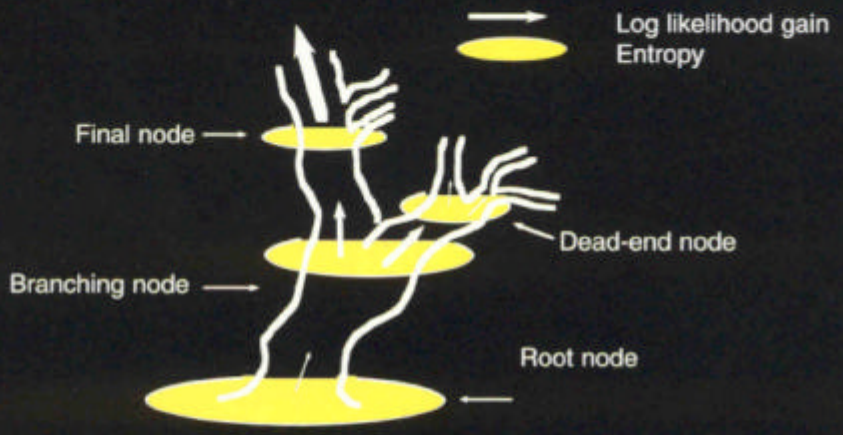

Statistical characterization of a "phasing tree"

TRANSACTIONS OF THE AMERICAN CRYSTALLOGRAPHIC ASSOCIATION
Volume 30, 1994

Editors
Gérard Bricogne and Charles W. Carter

TRANSACTIONS
OF
THE AMERICAN CRYSTALLOGRAPHIC ASSOCIATION

VOLUME 30 1994

Proceedings of the Symposium on

Likelihood, Bayesian, Inference and Their Application to the Solution of New Structures

at

Atlanta Convention Center
Atlanta, GA

June 25 - July 1, 1994

Editors

Gérard Bricogne
MRC
Laboratory of Molecular Biology
Cambridge, UK

Charles W. Carter
Dept. of Biochemistry & Biophysics
University North Carolina
Chapel Hill, NC 27599-7260

ISBN 0-937140-39-2
ISSN 0065-8006

Copies may be purchased from

Polycrystal Book Service
P.O. Box 3439
Dayton, OH 45401, USA

Table of Contents

ON THE SOLUTION OF THE MOLECULAR REPLACEMENT PROBLEM AT VERY LOW RESOLUTION: APPLICATION TO A RIBOSOME MODEL CRYSTAL

Alberto D. Podjarny, Alexandre G. Urzhumtsev*

UPR de Biologie Structurale, 15, rue Descartes, 67084 Strasbourg, France

**Permanent position: Institute of Mathematical Problem of Biology, Russian Academy of Sciences, 142292 Pushchino, Moscow Region, Russia*

Jorge Navaza

Laboratoire de Physique, Faculté de Pharmacie, 92290 Chatenay Malabry, France

The applicability of the Molecular Replacement (MR) method, implemented through the AMoRE package, is studied at very low resolution (d > 20 Å). Specific problems appear, mainly at the level of the translation function based on Patterson overlap. To solve these problems, this translation function is replaced by a systematic search using amplitude correlation. The corresponding algorithms are applied to two cases: the $tRNA^{Asp}$-RS complex (neutron diffraction data) and a ribosome model crystal (calculated data). This new implementation is shown to solve the problem for a variety of search models, ranging from a detailed atomic model to a rough envelope.

1. INTRODUCTION

The molecular replacement method has become a widespread and powerful technique for solving the phase problem when a structure closely related to the one under study (or a fragment of it) is available. This method is generally applied to diffraction data of 6 Å or higher resolution. A similar problem appears when an image of the structure under study is known at a much lower resolution, e.g., when an electron microscopy image of 30 to 50 Å is known, or when the search structure is not accurate enough and can provide only the molecular envelope.

The correct placement of such an image in the crystallographic unit cell is useful in several ways. For the case of a totally unknown structure, it provides a starting phase set for phase extension procedures, as well as the information (e.g., the molecular envelope, placement of NCS related units) necessary for some of these procedures. For the case when the model of an homologous structure is known, but it is significantly different, the placement of a low resolution envelope might provide the right solution when standard molecular replacement has failed.

The cubic form of the $tRNA^{Asp}$-synthetase complex provides an ideal case where the possibility of correctly placing an envelope can be tested, since:

a) a high resolution structure of the same complex is available [1], and therefore a search can be done with either model or envelope at different resolutions;

b) due to the high solvent content [2] the envelope is well defined inside the unit cell;

c) neutron data is available with excellent very low resolution completeness [3]

The work described below shows that indeed, it is possible to use very low resolution data to position an envelope. However, in order to do so current molecular replacement techniques need to be improved, since their direct application may fail to solve the problem. These improvements and their application to the cases of the $tRNA^{Asp}$-synthetase complex and of a ribosome model crystal are described below.

2. MOLECULAR REPLACEMENT STRATEGY

The methods herein developed are based on the MR package AMoRe [4]. The AMoRe package consists of the same steps of rotation function, translation function and rigid body refinement that conventional MR methods. Its main advantages are :

- it samples by using fast algorithms a much larger portion of six-dimensional space than conventional MR methods;

- there is a high degree of automation; for example, when many molecules need to be found within the asymmetric unit, the information coming from already located models is automatically incorporated into the procedure;

- several search criteria are used simultaneously;

- to improve speed, the main programs of the package do not use atomic coordinates but Fourier coefficients;

- the search models may be approximate electron densities such as molecular envelopes or images coming from electron microscopy.

The domain of potential orientations is sampled by the fast rotation function, which has several improvements over currently used ones, e.g. MERLOT [5] or XPLOR [6]. In particular, it is casted in the form of a correlation coefficient between truncated Patterson functions and the angular resolution of peaks is enhanced by skipping low angular resolution terms; furthermore, there is no limitation on the value of the integration radius, for a given data resolution. A large number of retained orientations are then used to compute translation functions. First a selection of peaks is made by computing the centred overlap of observed and calculated Patterson functions:

$$\text{Overlap} = \sum_h [I_{obs}(h) - \langle I_{obs} \rangle] \times [I_{calc}(h; \mathbf{R},\mathbf{t}) - \langle I_{calc} \rangle(\mathbf{R},\mathbf{t})] \quad (1)$$

which is computed from the amplitudes, both observed, Iobs(h), and calculated, Icalc(h; **R**,**t**), where **R** represents the three rotation parameters and **t** represents the three translation parameters. Another option of the package is the full-symmetry phased-translation function [7,8], which involves essentially amplitudes instead of intensities.

The output is however the full correlation function,

$$\text{Corr(F)}= \frac{\Sigma_h\,[\text{Fobs(h)}-\langle\text{Fobs}\rangle]\ \text{x}\ [F_{calc}(h;\,\mathbf{R},\mathbf{t})-\langle F_{calc}\rangle(\mathbf{R},\mathbf{t})]}{\{\Sigma_h\,[F_{obs}(h)-\langle\text{Fobs}\rangle]^2\}^{1/2}\ \text{x}\ \{\Sigma_h[F_{calc}(h;\,\mathbf{R},\mathbf{t})-\langle F_{calc}\rangle(\mathbf{R},\mathbf{t})]^2\}^{1/2}} \qquad (2)$$

defined in terms of amplitudes, Fobs(h) and $F_{calc}(h;\,\mathbf{R},\mathbf{t})$, and calculated for the top peaks of the overlap function. The final list, sorted in descending order of correlation, includes also the R-factor.

It has been observed that in general high overlaps correspond to high correlations, so that only a rather small number of peaks are retained for each orientation. However this is not a general rule, and sometimes the greatest correlation may correspond to a peak which has a very low rank in overlap. This is particularly true for the present studies (see section 3.3). Eventually the **R, t** parameters are refined by a fast rigid body refinement procedure.

In the case where many molecules or fragments have to be located within the asymmetric unit, the contribution of the best n-body solution is used to compute (n+1)-body translation functions.

AMoRe has proven very effective in solving the MR problem at high and medium resolution ranges, and therefore its parameters are tuned accordingly. Since the nature of the signal varies when lowering the resolution range, the nature of the function used to detect it should vary also. The purpose of this paper is to develop the necessary changes to make AMoRe work at very low resolution ranges.

3. LOW RESOLUTION MR. TESTS WITH AN ATOMIC MODEL

3.1 Initial check of standard AMoRe protocol.

To develop the low resolution protocols, the neutron data from the cubic form of the $tRNA^{Asp}$-RS complex was used [3]. This structure was solved by AMoRe using the standard protocol, a high resolution model from a different crystal form [1] and X-ray diffraction data at 8 Å resolution [9]. The solution showed very clearly one single dimer in the asymmetric unit, placed in a general position.

During the initial stages of the solution of this structure [10], neutron data had been collected in the resolution range ∞-20 Å for three different D_2O/H_2O contrasts, corresponding to the diffraction of the tRNA, the synthetase and the full complex , respectively [3]. This data is very complete to 26 Å; moreover, the number of reflections (31) at 50 Å resolution is enough to have a significant observations/parameters ratio in a six-dimensional search.

To test the power of the standard protocol of AMoRe at low resolution, several searches with the complex dimer were conducted using the neutron diffraction data from the full complex from 20 Å to infinity (although the high resolution end is not complete). These searches gave no solution when using the centred-overlap translation function, even when all positive peaks were considered. Although for the best positions the value of Corr(F) after refinement was high (max = 81%), the R-factor was systematically too high (min = 47%) and no position was close to the correct one. Moreover, the peaks of the translation function correspond to positions where the dimer is placed on a rotation axis, and even on the origin of the cubic space group. The reason for this failure is not the quality of the neutron data, since a comparison of the experimental neutron diffraction data and the model data from correct solution gives a Corr(F) of 92% and an R-factor of 28.3%. This check shows that very low resolution data can be accurately calculated from a model, which is therefore a proper search object. Therefore, the problem is that in this case the use of the centred Patterson overlap as the translation function missed the global maxima of the correlation function between F_{obs} and $F_{calc}(h;\,\mathbf{R},\mathbf{t})$, which certainly would be present in a full six-dimensional search.

It should be noted that the standard protocol did give the correct solution when using the full-symmetry phased-translation function, but the peak for the correct position (which has the largest full correlation factor, see formula (2)) appeared beyond the 50th position of this phased-translation function. Therefore, this procedure could also miss the right solution if only the top peaks of the translation function were investigated, as is usually the case .

3.2 Tests with calculated diffraction data

In order to find the right protocol for searches at low resolution, diffraction data calculated from the atomic model without solvent modelization were used at various resolution ranges. The use of model data is needed in the first stages to avoid the effect of the error in the amplitudes or of their lack of completeness.

Since the overall resolution range is considerably wider than the one available from the experimental data, several intermediate resolution ranges could be tested (d_{min} varied from 8 to 30 Å, d_{max} varied from 15 Å to infinity). The original AMoRe protocol works for almost all cases. For example, in the 15-30 Å resolution range, the rotation error is 6° for the first peak (height = 18.6) and 25° for the second peak (height = 14.6), and after translation searches and refinement the correlation in F is 96% for the first peak, which is correct, and 48% for the second peak, which is wrong.

However, there are two exceptions:

a) When the higher resolution limit is lower than 30 Å, the rotation function has a large error (about 20°), which causes overall failure. This poses a major problem for the use of envelopes as a search object.

b) When the "inner core" of reflections (d > 50 Å) are included, the translation function based on Patterson overlap fails even for cases were the rotation function has worked nicely (5° error). This arises from the fact that the Patterson overlap is not properly normalized and is dominated by a few ultra-low resolution very strong terms.

Unfortunately, problem (b) precludes the use of the "central reciprocal space zone" terms to diminish the sensitivity of the translation searches to errors in the rotation parameters, which causes problem (a).

The solution of these problems could not be done by simple adjustments of the existing protocol but needed the development of a new one, based on correlation functions instead of Patterson overlap.

3.3 Development of a new protocol. Model data

To solve the problem highlighted above, search programs [11] which use directly as the target value the correlation of amplitudes (F or F^2, see formula (2)) were used instead of the Patterson overlap. The difference of these two functions is specially evident when the values of F_{calc} are strongly dependent of the rotation and translation parameters. This is the case for very low resolution reflections, where the value of F_{calc} will increase considerably when the molecules overlap with their symmetry related images. Since the Patterson overlap has F_{calc} only in the numerator (formula 1), its value will increase artificially when molecules overlap. For the correlation, where F_{calc} appears both in the numerator and the denominator (formula 2), this effect is cancelled.

This strategy has solved the cases which had previously failed, provided that the translation searches were done at the resolution of 50Å-∞. All cases confirm the previous observation that the translation searches using the lowest resolution ranges and based on correlation functions show the

signal clearly, even with large rotation errors. These errors are corrected in the refinement step. For example, for the resolution range 50Å-∞, this procedure corrected an initial rotation error of 20° (second peak of the rotation function) to end after refinement with a correlation of 99%, a rotation error of 2° and a translation error of 1 Å. The correlation in F worked slightly better than the correlation in F^2.

Further tests showed that the rotation error limit for correct translation searches usually lies around 20°. However, the rotation error can be as large as 30°, particularly when the data used goes only to 40 or 50 Å. To assure that the error in the rotation parameters is small enough to fall within the 20° limit, a scanning with a step of ±20° around the rotation peaks was introduced. The peak with its neighbourhood of ±20° is called the "expanded rotation peak".

This protocol was also applied to a model case at 50 Å resolution, where the Patterson radius was displaced on purpose from the optimal value. This increased the rotation error from 20° to 27°, but even this larger value could be corrected by using the "expanded rotation peak" as input to the translation function and the refining with the "inner core" reflections.

3.4 Tests with experimental neutron diffraction data

In order to test the protocol using real diffraction data, the same procedure was applied for the experimental neutron data at very low resolution. It converged to the correct solution in all cases. As before, the limitation of data at the high resolution end causes a large error (27°) in the rotation function, but the translation search and rigid body refinement give the correct solution and correct the rotation error. For the final solution, the Corr(F) value was 97%, the rotation error was 2° and the translation error was 1Å.

When some of the parameters (e.g., Patterson radius) are changed, the rotation function finds a position with larger error (28°), enough to cause failure of the translation function. In this case the expansion of rotation peaks is necessary, and it finds the right solution.

3.5 Summary of searches with an atomic model.

The low resolution searches described above show that different resolution ranges should be used for different types of searches. For rotation searches the highest available resolution is preferable, and very low resolution terms can be excluded. Translation searches should be done using correlation searches against very low resolution data. The neighbourhood of rotation peaks should be explored. Rigid body refinements should be done against all available data. However, using the lowest resolution data may be important for correcting large errors, even when it may also lower the signal/noise contrast (for example, the ratio of the correlation for the correct and the first false peaks are 99% / 87% at the resolution 30Å-∞ against 98% / 63% for 30-40Å).

4. TESTS WITH ENVELOPES

The object available for conducting low resolution searches might be an envelope (and not a detailed atomic model), for example coming from electron microscopy or from very approximate models. Therefore it is important to check whether the protocol described above can be used to correctly place a molecular envelope inside the unit cell.

Preliminary tests on structures solved at high resolution [12] have shown that at a resolution lower than 15 Å there is good correspondence between the observed diffraction amplitudes and the ones calculated from envelopes. This limit is necessary since at higher resolution (10 to 15 Å) the

solvent region cannot be considered flat, and therefore the diffraction amplitudes have a significant solvent contribution.

As before, the studies with envelopes were conducted using the neutron data from the cubic form of the $tRNA^{Asp}$-synthetase complex.

4.1 Exact flat envelope, 50Å neutron data

To obtain an exact envelope, each atom of the model was surrounded by a ball of 2.5Å radius. For the purpose of using AMoRe, the resulting points were placed in a box 6 times larger than the model in each linear direction, where it occupied 0.0012 of the volume, and assigned a density value of 1; the rest of the points are set to 0. This density was then used to calculate structure factors. The R-factor at 50Å between modules from the atomic model and from this flat envelope was equal to 4%. This shows that at this low resolution range, the transform of an atomic model is virtually the same as that of the corresponding exact envelope. The protocol optimised using the searches with a model was used, and the results were, as expected, virtually the same as those obtained using an atomic model.

4.2 Density-based envelope, 50Å neutron data

To obtain a more realistic envelope, the model structure factors were used to calculate a density distribution at 50Å, which was placed in the same box as before. The envelope is defined by all the points above a cutoff level. In this synthesis, the envelope can be expanded to 0.0035 of the volume by lowering the cutoff level before it includes noise peaks.

Two possibilities were considered: a flat envelope or a modulated one, where the density values inside the molecular envelope are kept. For both cases, two different cutoff levels were considered, corresponding to the exact molecular volume and to three times the molecular volume. It was found that for the flat envelope the exact molecular volume fits the data better (R-factor is 15% against 39%), while for the modulated envelope the larger molecular volume is better (31% against 12%).

Searches were done using both the flat and the modulated envelopes at their optimal volumes. The solution was clearly found for both cases. Again, the orientation errors are large (17° and 18°, respectively) but they are within the rotation peak expansion.

4.3 Modulated envelope; 20Å neutron data

These tests were repeated at higher resolution. The model structure factors were used to calculate a density distribution at 20Å. In this synthesis, the envelope can be expanded to 0.0020 of the volume by lowering the cutoff level before it includes noise peaks. Like in the 50 Å case, for the flat envelope the exact molecular volume fits the data better (R-factor is 14% against 37%), while for the modulated envelope the larger molecular volume is better (29% against 11%). Searches were conducted using the modulated envelope only, and the correct solution is found. It should be noted that the signal contrast here is higher than in the 50Å-resolution searches (the ratio of the correlation of the correct peak to the first false one is 84% / 81% at 50Å and 96% / 84% at 20Å).

4.4 Protocol for low resolution searches with envelopes

From this work the following rules can be derived:

1) To get a search model, a synthesis should be calculated, then cut at the "noise level" (1-3 times larger than the atomic model volume);

2) The same procedure of MR which was used for atomic models at very low resolution can be applied also for envelopes;

3) Both modulated and flat envelopes work; however, modulated envelopes are less dependent on an exact definition of the cutoff level.

5. TESTS ON RIBOSOME MODEL DATA

A case where finding the position and orientation of an envelope is very important is that of the ribosome particle. Previous to applications with measured experimental data, it was necessary to test the ideas described above. These tests have two objectives: to confirm the results of the experiences with the tRNA-synthetase complex in a different case, and to find the best parameters to be applied in the ribosome case. To do so, a model was constructed for the tetragonal crystal form of the 50S particle (T50S, space group $P4_12_12$, a=b=498, c=198 Å) for *Thermus Thermophilus* [13]. It was based on an 28 Å EM image of *Bacillus Stearotermophilus* (B50S), provided by A. Yonath and coworkers [14]. This image was obtained using diffraction information from tilt-series of two-dimensional crystalline arrays. It provided an envelope, which was packed in the tetragonal crystal lattice observed for the T50S particles. This artificial packing simulated proper crystalline contacts. Structure factors were calculated from this model crystal at 20Å resolution.

5.1 Low Resolution MR Runs On Simulated Ribosome Data

Table 1 shows that the application of the protocol described above for the tRNA-synthetase complex finds immediately the right solution with a very high contrast. This is not surprising, since the data has no errors and the model is perfect. Note that in this perfect case there was no need to use either the highest resolution terms for the rotation function nor the very low resolution terms in the translation correlation searches.

TABLE 1

	Resolution	function.	1	2	3
Rotation	30-50 Å	Peak height	8.9	6.4	5.9
		error(°)	0.5	36.8	44.6
Translation	20-50 Å	Corr(F)	95.0	31.4	31.8
		Signal in σ	18.9	4.9	4.7
		error(Å)	1	51	32
Refinement	20-50 Å	Corr(F)	98.4	33.9	31.3
		R-factor	7.9	53.5	53.2
		error	0.°, 0Å		

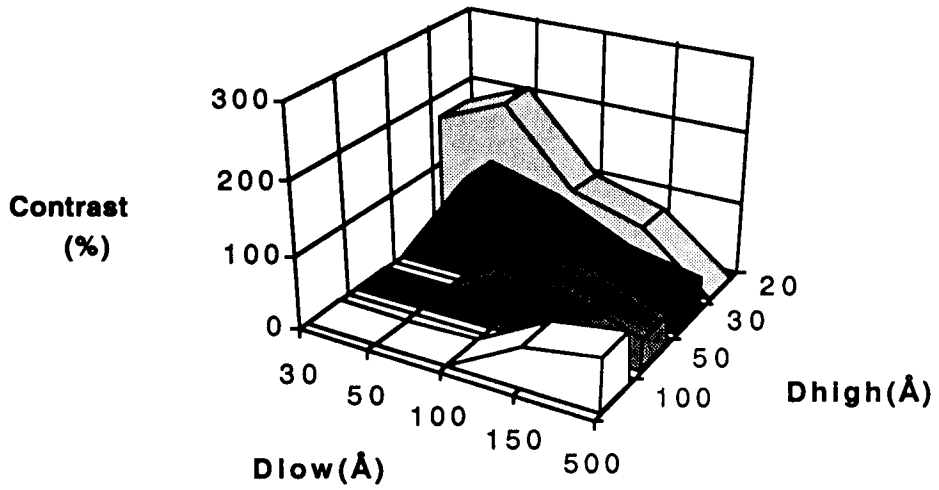

Figure 1a. The contrast (height of first correct peak/height of first wrong peak) of the rotation function, as a function of the resolution range of the data. A contrast value >100% means that the first peak of the rotation function is correct; a lower one means that the correct peak appears, but not as the first one. Forbidden ranges (Dlow<= Dhigh) have a zero value.

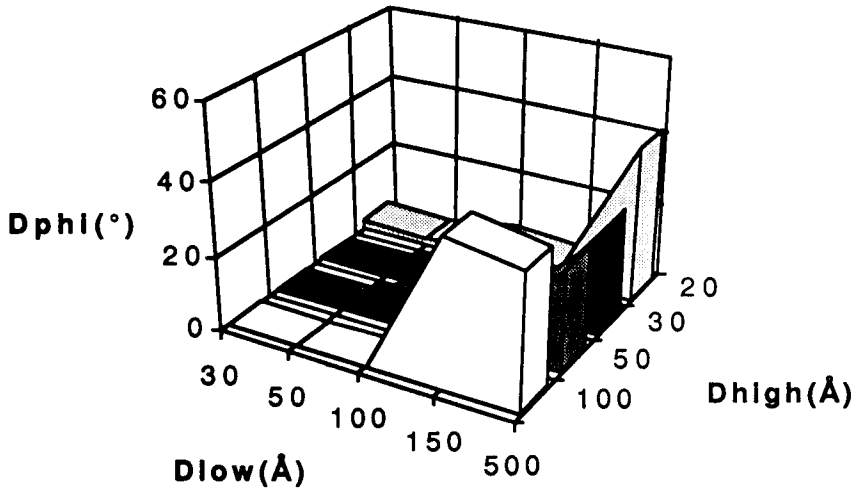

Figure 1b. The error (Dphi) measured as the angular distance between the rotation function peak and correct rotation values, as a function of the resolution range of the data. Forbidden ranges (Dlow<= Dhigh) have a zero value.

5.2 Systematic Study Of Signal/Noise Ratio And Tolerance To Errors

In order to optimize the parameters for the different steps of MR, a systematic analysis was done for each of them. The most crucial variable is the resolution range (Dhigh-Dlow cut-offs); therefore the searches were repeated systematically for a wide variety of them.

a) Rotation Functions.

Rotation functions were conducted varying both ends of the resolution range. The highest resolution (Dhigh) was varied between 20 and 100 Å, and the lowest resolution (Dlow) was varied between 30 and 500 Å. In each case the ratio (contrast) of the height of the "correct" peak to that of the first wrong peak was calculated (see figure 1a) and the error (Dphi) of the "correct" peak was noted (see figure 1b).

This analysis confirms the previous observations that the best contrast is obtained using the highest possible resolution and without the inner core of reflections, and that the error of the rotation peaks increases when the inner core of reflections is included.

b) Translation Functions

Translation functions were calculated also for a wide range of resolutions. In this case, an additional dimension was added: the error in the orientation of the input model, which was varied from 0 to 40°. Figure 2 shows the behaviour of the signal/noise ration for the cases of 0° rotation error and 30° rotation error. If the error is less than 20°, the best resolution range is the highest one, and the introduction of the inner core of reflections lowers the contrast (figure 2a). If the error is larger than 20°, including the inner core of reflection becomes crucial for finding the solution. However, the price is decreasing contrast (figure 2b).

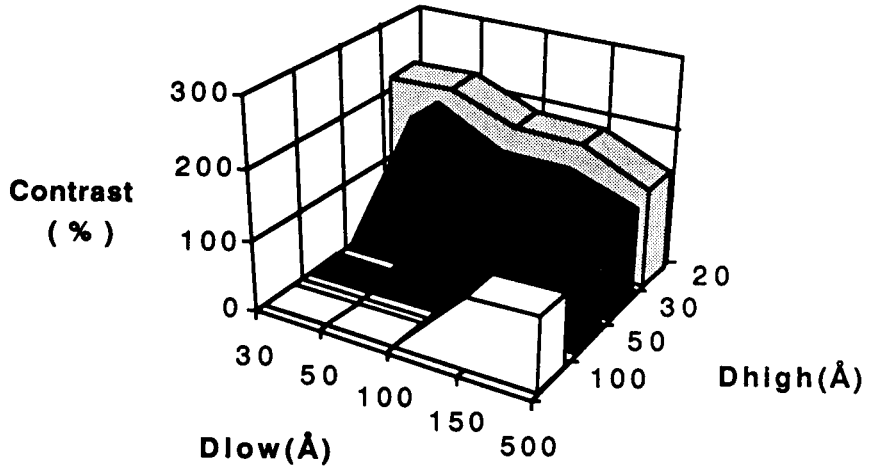

Figure 2a. Contrast of the translation function for 0° rotation error. Forbidden ranges (Dlow≤ Dhigh) have a zero value.

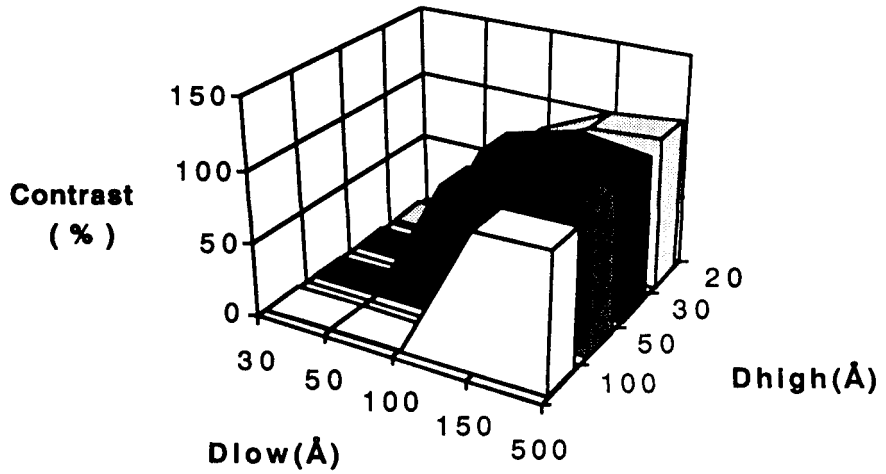

Figure 2b. Contrast of the translation function for 30° rotation error. Forbidden ranges (Dlow≤ Dhigh) have a zero value.

c) Refinement

Since the role of this step is mainly to correct rotation and translation errors, the maximum allowable translation error (DXmax) was analyzed as a function of resolution range and of orientation error. This analysis is shown in Figure 3.

Figure 3a shows the results for 0° rotation error and figure 3b those for 30° rotation error. In general, the radius of convergence was very high (up to 30° and 30 Å). However, for high rotation error the inclusion of the reflections in the 20-30 Å resolution range causes overall failure.

6. CONCLUSIONS

This study highlights the importance of the use of correlation functions directly as the search criterion. It also shows that, in the very low resolution case, the optimum resolution ranges are not the same for the rotation function, the translation function and the refinement steps. The rotation function works best using higher resolution terms; but for experimental data the errors in rotational parameters are large. The correlation searches and subsequent refinement based on the lowest resolution data only are capable of correcting this error. In some cases, the rotation error is too large and the rotation peak needs to be expanded to fall within the radius of convergence of the translation and refinement procedures. The low resolution case is therefore a particular one, and needs the change of the standard protocol according to these rules. With these changes, MR packages (e.g., AMoRe) can be used successfully to solve the molecular replacement problem at very low resolution.

The experience gained in the atomic model searches has been applied to searches with molecular envelopes. These searches are very important since they open a whole new field, that of using experimentally determined envelopes as the search model in the MR procedure. We have been able to solve this problem for the case of the cubic $tRNA^{Asp}$-synthetase complex. The behaviour of the envelope searches is similar to that of searches using the atomic models. Thus, this work has succeeded in finding a molecular replacement protocol that can use envelopes as the search object at very low resolution.

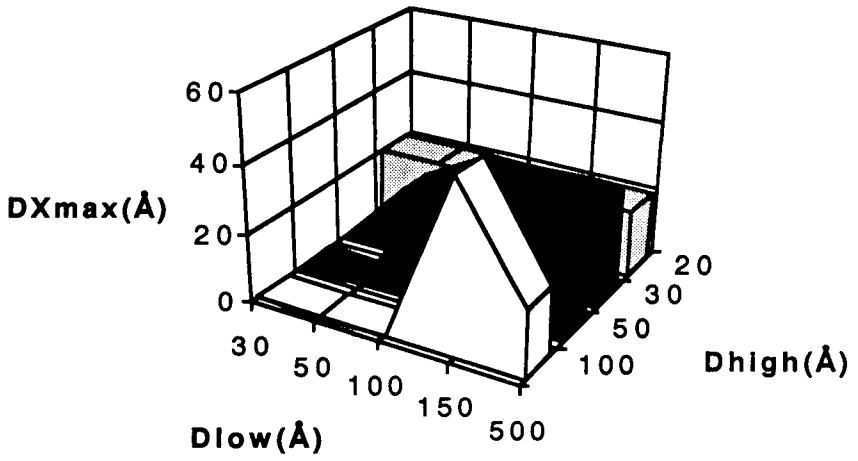

Figure 3a. Maximum allowed translation error for 0° rotation error. Forbidden ranges (Dlow≤ Dhigh) have a zero value.

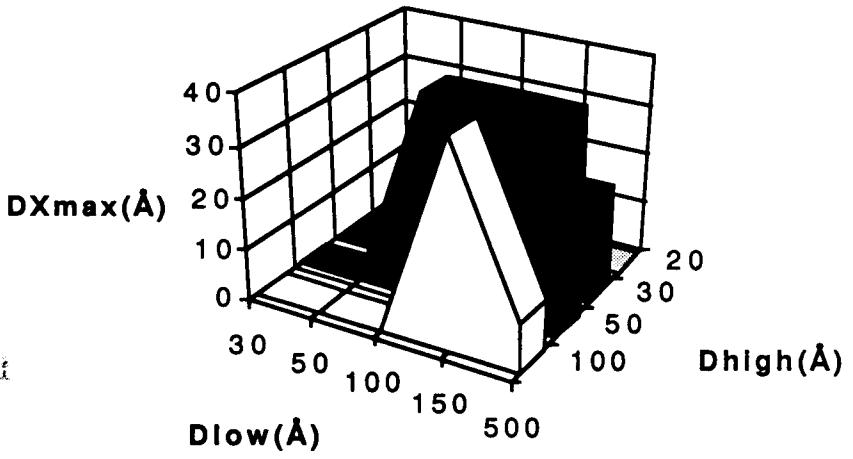

Figure 3b. Maximum allowed translation error for 30° rotation error. Note that the inclusion of reflections between 20 and 30 Å causes failure of the refinement. Forbidden ranges (Dlow≤ Dhigh) have a zero value.

This experience is currently being applied to the case of the ribosome, both for simulated ribosome crystals and experimental X-ray diffraction data. The first part of this work, concerning tests with a ribosome model crystal, shows clearly that the rules developed from the experience with the tRNA-RS complex are more generally applicable. Following these tests, we applied the protocol to experimental data. The results so far are encouraging, and will be published elsewhere.

ACKNOWLEDGEMENTS

The experimental data of the $tRNA^{Asp}$-synthetase complex used in this work were collected by Drs. J.Cavarelli, J.-C.Thierry and D.Moras (X-ray data) and by Drs. M.Roth, A.Lewitt-Bentley and D.Moras (contrast variation neutron data). We thank them for making these data available to us. The EM image used for generating the ribosome model crystal was provided by Dr. A. Yonath and coworkers; we thank them for making these data available to us, and for continuous discussions and encouragement. We also thank Dr. B.Rees for useful discussions and making available all his previous work on the different aspects of the crystallography of the cubic form of the $tRNA^{Asp}$-synthetase complex and Dr. P.Dumas and Dr. M. Roth for their continuing interest and encouragement on the current work. This work is supported by the CNRS through the UPR 9004, and by EMBL through a fellowship to A.G.U.

REFERENCES

[1] M Ruff, S. Krishnaswamy, M. Boeglin, A. Poterszman, A. Mitschler, A. Podjarny, B. Rees, J.-C. Thierry & D. Moras, *Science* 252 (1991), 1682.

[2] B. Lorber, R. Giegé, J.-P. Ebel, C. Berthet, J.-C. Thierry & D. Moras, *J. Biol. Chem.* 258 (1983), 8429.

[3] D. Moras, B. Lorber, P. Romby, J.-P. Ebel, R. Giegé, A. Lewit-Bentley, & M. Roth, *J. Biomol. Structure & Dynamics* 1 (1983), 209.

[4] J. Navaza , *Acta Cryst.*, A50 (1994), 157.

[5] P.M.D. Fitzgerald, *J. Appl. Cryst.* 21 (1988), 273.

[6] A.T. Brünger, J. Kuriyan & M. Karplus, *Science* 235 (1987), 458.

[7] P.M. Colman, H. Fehlhammer & K. Bartels In *Crystallographic Computing Techniques,* eds. F.R. Ahmed, K. Huml & B. Sedlacek, (Copenhagen, Munksgaard 1974), p 248.

[8] G.A. Bentley & A. Houdusse, *Acta Cryst.* A48 (1992), 312

[9] A.G. Urzhumtsev, A.D. Podjarny & J. Navaza, 30, CCP4 Newsletter (1993), 29.

[10] A.D. Podjarny, B. Rees, J.-C. Thierry, J. Cavarelli, J.C. Jesior, M. Roth, A. Lewitt-Bentley, R. Kahn, B. Lorber, J.-P. Ebel, R. Giege & D. Moras, *J. Biomol. Struct. & Dynamics* 5 (1987), 187.

[11] A.G. Urzhumtsev. & A.D. Podjarny, *J. Appl. Cryst.* 27 (1994), 122.

[12] A.G. Urzhumtsev. & A.D. Podjarny, *Réunion Francophone de Crist. de Macromol., Ste-Odile, 2-5 Juin 1993*, Abstract A1.

[13] A. Yonath, *Ann. Rev. Biophys. Biomol. Struct.* 21 (1992), 77.

[14] A. Yonath, K.R. Leonard & H.G. Wittmann, *Science* 236 (1987), 813.